



## Investigation of mixed mode - I/II fracture problems - Part 1: computational and experimental analyses

O. Demir

*Department of Mechanical Engineering, Sakarya University, 54187, Sakarya, Turkey*

*Department of Mechanical and Manufacturing Engineering, Bilecik Seyh Edebali University, 11230, Bilecik, Turkey*  
*oguzhan.demir@ogr.sakarya.edu.tr*

S. İriç

*Department of Mechanical Engineering, Sakarya University, 54187, Sakarya, Turkey*

*siric@sakarya.edu.tr*

A. O. Ayhan

*Department of Mechanical Engineering, Sakarya University, 54187, Sakarya, Turkey*

*ayhan@sakarya.edu.tr*

H. Lekesiz

*Department of Mechanical Engineering, Bursa Technical University, 16190, Bursa, Turkey*

*huseyin.lekesiz@btu.edu.tr*

**ABSTRACT.** In this study, to investigate and understand the nature of fracture behavior properly under in-plane mixed mode (Mode-I/II) loading, three-dimensional fracture analyses and experiments of compact tension shear (CTS) specimen are performed under different mixed mode loading conditions. Al 7075-T651 aluminum machined from rolled plates in the L-T rolling direction (crack plane is perpendicular to the rolling direction) is used in this study. Results from finite element analyses and fracture loads, crack deflection angles obtained from the experiments are presented. To simulate the real conditions in the experiments, contacts are defined between the contact surfaces of the loading devices, specimen and loading pins. Modeling, meshing and the solution of the problem involving the whole assembly, i.e., loading devices, pins and the specimen, with contact mechanics are performed using ANSYS™. Then, CTS specimen is analyzed separately using a submodeling approach, in which three-dimensional enriched finite elements are used in FRAC3D solver to calculate the resulting stress intensity factors along the crack front. Having performed the detailed computational and experimental studies on the CTS specimen, a new specimen type together with its loading device is also proposed that has smaller dimensions compared to the regular CTS specimen. Experimental results for the new specimen are also presented.

**KEYWORDS.** Fracture; Mixed Mode; Mode-I/II; Compact Tension Shear; Finite Element Method.

## INTRODUCTION

Although many fracture mechanics problems seen in practice can adequately be analyzed by taking into account only mode-I conditions, there are still many problems that are subjected to mixed mode loading, for which mode-I analysis approaches are not sufficient. The mode mixity of the problem can be due to orientation of an initial defect existing in the structure caused by imperfections or processes such as manufacturing operations. Another source of mixed mode loading on the crack is due to the nature of loads that exist on the structure. For such situations, analyses of the cracked structure under mixed mode loads and related criteria for fracture conditions are needed. The most basic type of mixed mode fracture is mode-I/II, in which both mode-I (opening) and mode-II (shearing) loads act on the crack tip. There are various studies and criteria that exist in the literature for mixed mode-I/II fracture. Maximum tangential stress (MTS) criterion [1], minimum strain energy density (SED) criterion [2], maximum energy release rate (MERR) criterion [3, 4], maximum tangential strain criterion (MTSN) [5] are some of the most common criteria used to understand the fracture behavior of materials under mixed mode-I/II loading conditions. Koo and Choy [6], Pook [7] and Tanaka [8] also proposed different criteria for in-plane mixed mode problems. Numerous experimental and numerical analyses were performed and various types of specimens [9-11] were introduced by researchers and used in experimental analyses. Richard also performed many detailed and comprehensive studies using new and modified CTS specimen and proposed new criteria that includes empirical formulations involving  $K_I$ ,  $K_{II}$ , equivalent stress intensity factor (SIF) and crack deflection angle separately [12-14].

In this study, results from finite element analyses of the test system composed of compact tension shear specimen, loading apparatus and pins are presented. Using the results from analyses of the assembly for different load mixity angles for the specimens, corresponding fracture analyses are also performed on the specimen submodel and mixed mode stress intensity factors computed. Results from experimental studies on a new type of specimen, called T-specimen, which has smaller dimensions and requires less material, are also presented. Fracture experiments of the finite element models of CTS and T specimen are also conducted to check the validity of some of the existing criteria for mixed mode-I/II fracture conditions and to develop a further refined mode-I/II fracture criterion (Part 2).

The outline of the paper is as follows: In the next section, details of the finite element models including fracture submodels are given. This is followed by description of the test procedure and the corresponding experimental results. Finally, preliminary fracture results from a new type of mixed mode specimen are presented.

## FINITE ELEMENT MODELING OF MODE-I/II FRACTURE

In this section, details and results of the finite element models of CTS specimen are presented. First, finite element models, boundary conditions and loads are described. In the second subsection, results of the finite element models in terms of stress intensity factors are presented.

### Description of Finite Element Models

In Fig.1, overall and exploded views of the mixed mode-I/II test assembly solid model for  $0^\circ$  loading angle and finite element model and dimensions of CTS (compact tension shear) specimen are shown. As can be seen in Fig.1 (a), mixed mode loading clevises are designed to allow the loading axis to pass through the specimen center under different loading angles ( $0^\circ$ ,  $15^\circ$ ,  $30^\circ$ ,  $45^\circ$ ,  $60^\circ$ ,  $75^\circ$ ,  $90^\circ$ ). CTS specimen proposed by Richard [13] is used in fracture analyses and experiments (Fig. 1 (b)).

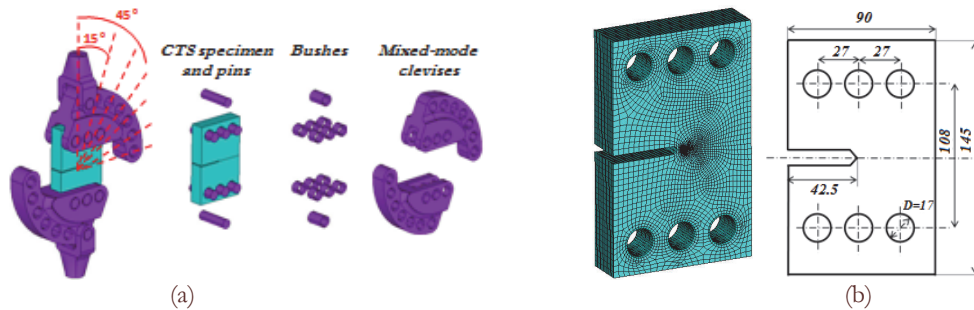


Figure 1: Overall and exploded views of the mixed mode-I/II test assembly solid model and finite element model and dimensions of CTS specimen.



Modeling, meshing, defining loads, boundary conditions and contacts and the solution of the problem involving the whole assembly, i.e., loading devices, pins and the specimen, with contact mechanics are performed using ANSYS™ [15]. To simulate the real conditions in the experiments, contacts are defined between the contact surfaces of the loading devices, bushes, specimen and pins (Fig. 2).

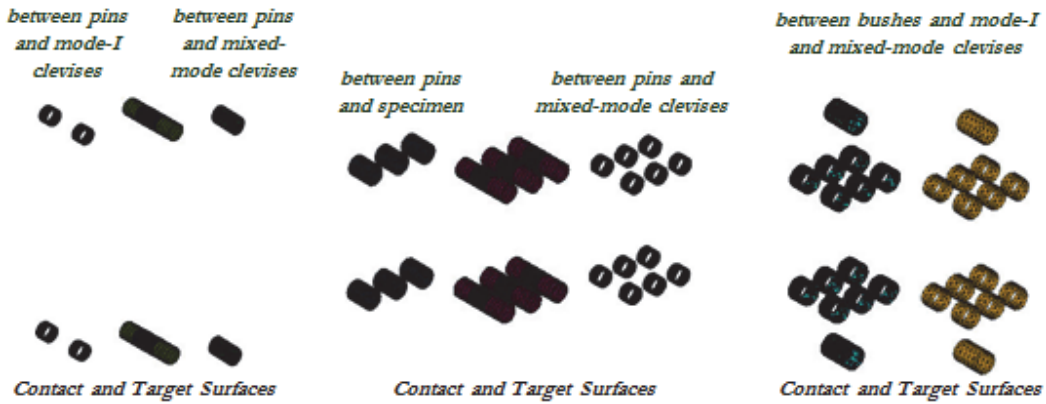


Figure 2: Contact and target surfaces between the mode-I clevises, mixed-mode clevises, bushes, specimen and pins.

Also to provide the real conditions of experiments, boundary conditions are defined such that the bottom mode-I clevis surface nodes are constrained in all directions and the upper mode-I clevis surface nodes are allowed to move along loading axis only (Fig. 3). Load is applied on the upper loading clevis. Representative picture given in Fig. 3 is for 75° loading angle.

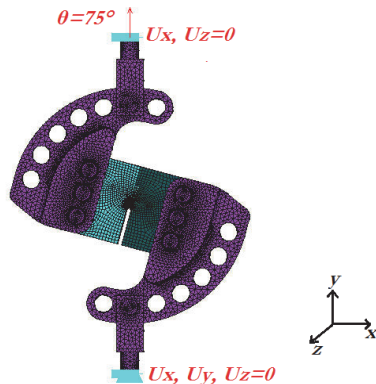


Figure 3: Boundary conditions and loading on mode-I/II test system – loading angle 75°.

Having obtained the overall solution using ANSYS, displacements are taken from nodes of the specimen loading hole surface by using submodeling. Then these displacements are applied on the specimen model, which is used in FRAC3D solver to calculate the resulting stress intensity factors (Fig. 4).

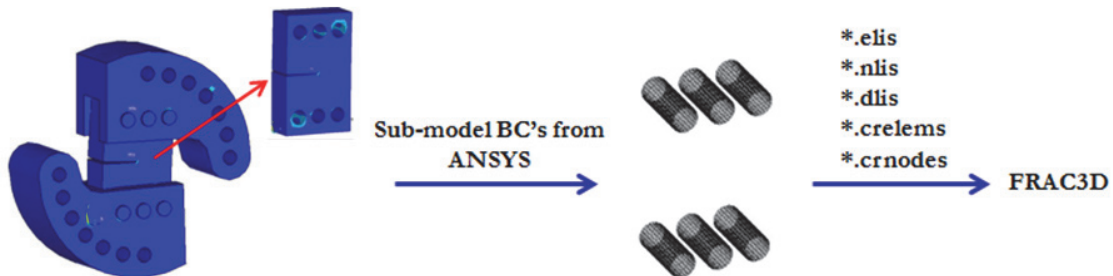


Figure 4: Applying the submodeling approach and transfer of the specimen and crack tip node and element files to FRAC3D.

FRAC3D, a general-purpose finite element based 3-D fracture analysis program, employs enriched crack tip elements to compute the stress intensity factors. The enriched finite elements do not require special mesh near crack front and stress intensity factors are directly solved for at the same time as nodal displacements without any post-processing effort. Further technical details related to three-dimensional enriched elements are given in [16, 17]. 25 mm-thick CTS specimens are used during the preliminary design stage of mixed-mode clevises. Results of stress and fracture analyses of CTS specimens (25 mm thick) for all loading angles showed that required loads to fracture the specimens (25 mm thick) are very high especially for highly mode-II conditions ( $60^\circ$ ,  $75^\circ$  and  $90^\circ$ ). Therefore, 10 mm-thick specimens are used in experimental analyses.

Some sensitivity analyses were performed in a previous study [18] to investigate the effect of boundary conditions and loads, contact type and friction coefficient between contact surfaces used in the analyses on the computed SIFs. The results from this study is summarized in Fig. 5. Firstly analyses were performed to check the linearity between the increment of applied loads on the clevises and the increment of stress intensity factor (Fig. 5 (a)). It can be clearly seen from the figure that there is a linear relation between the SIFs and the applied loads in the range considered. Frictional (0.2 friction coefficient), no separation, bonded and bonded (always) contact types were used respectively (Fig. 5 (b)) and also different friction coefficients (0.1, 0.2, 0.3 and 0.4) were used (Fig. 5 (c)) under constant loading angle (45 degrees) and load value (10 kN) to investigate the contact type effect on SIFs. Results showed that nearly there is no difference between the different cases of contacts and SIFs along the crack front are almost identical between the analyses with different friction coefficients. In Fig. 6, a process map is given to summarize the analysis procedure.

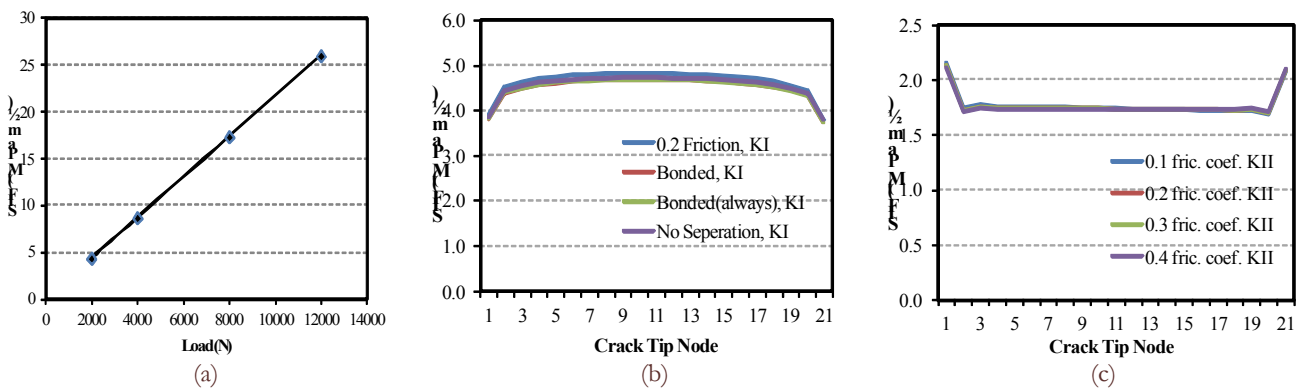


Figure 5: Sensitivity analyses to investigate the effect of (a) boundary conditions and loads, (b) contact type and (c) friction coefficient between contact surfaces used in the analyses on the computed SIFs.

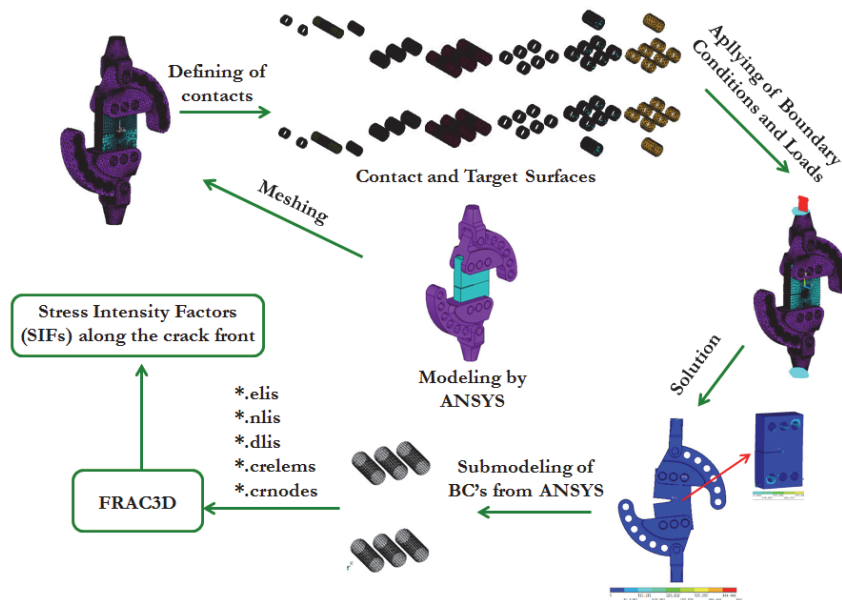


Figure 6: Process map of the analysis procedure.



### Results of Finite Element Models

In this subsection, results from mixed mode fracture analyses are presented for different loading angles. Tab. 1 summarizes results of fracture analyses from specimens with 43.5, 45, 47 mm crack lengths for 0°, 15°, 30°, 45°, 60°, 75°, 90° loading angles. 10 kN constant load is applied for all analyses. Analyses are also performed for 43.5 and 47 mm crack lengths, since fatigue pre-crack lengths measured after experiments are not always 45 mm. Using the additional analyses with different crack lengths, KI, KII and KIII SIF values corresponding to actual crack length obtained from experiments can be calculated by interpolation. In Fig. 7, variation of SIFs for 43.5, 45 and 47 mm crack lengths as a function of loading angles is given. 0° loading case i.e. mode-I loading case, is obtained by applying the load to the upper and lower left holes of the specimen using the axial loading clevis only. However load is applied to other holes of the specimen using mixed-mode clevises. Therefore, there is a high degree of change for KI SIF values between 0° and 15° loading angles.

Loading Angle (°)	43.5 mm Crack Length			45 mm Crack Length			47 mm Crack Length		
				SIFs into the crack front, (MPa·m <sup>1/2</sup> )					
	KI	KII	KIII (Edge Value)	KI	KII	KIII (Edge Value)	KI	KII	KIII (Edge Value)
0	8.78	0.00	0.00	9.13	0.00	0.00	9.59	0.00	0.00
15	4.37	0.32	0.11	4.60	0.46	0.16	5.13	0.43	0.18
30	3.91	0.65	0.22	3.91	0.82	0.24	4.59	0.94	0.33
45	3.16	0.94	0.35	3.17	1.18	0.36	3.74	1.35	0.45
60	2.23	1.15	0.40	2.20	1.48	0.50	2.63	1.72	0.57
75	1.05	1.30	0.46	1.10	1.67	0.51	1.31	1.94	0.63
90	-	-	-	0.00	1.73	0.55	-	-	-

Table 1: KI, KII and KIII stress intensity factors for different loading angles and crack front length.

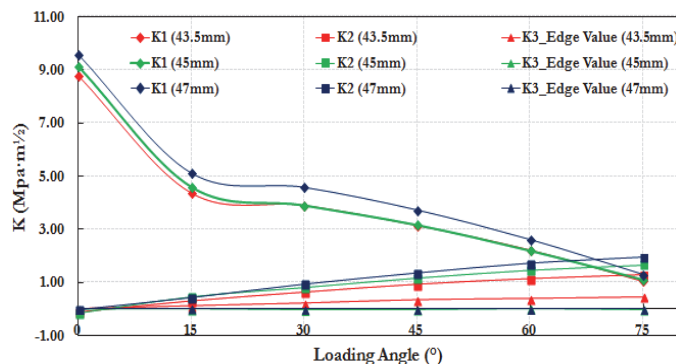


Figure 7: Variation of SIFs for 43.5, 45 and 47 mm crack lengths as a function of loading angles.

Stress distributions of mixed mode-I/II clevises, pins, bushes and specimen obtained from the analyses which is performed for 45 mm crack length under 10 kN load and 45° loading angle are given in Fig. 8. Furthermore, KI, KII and KIII SIFs along crack front are given in Fig. 9 (a). Stress distributions must be evaluated together with SIF values along the crack front obtained from the fracture analyses to provide small scale yielding conditions under LEFM (Linear Elastic Fracture Mechanics) rules. Although loading case is mode-I/II due to the Poisson's ratio, KIII SIF values are observed from analyses. Edges of upper and lower crack surfaces before and after applying the load are plotted in Fig. 9 (b). Owing to the applying load, upper crack surface is exposed to compressive stress and lower crack surface is exposed to tensile stress along the crack length direction. Thus, transverse expansion and contraction occur on the upper and lower crack surfaces, respectively. Consequently, this relative deformation between the upper and lower crack surfaces causes positive and negative tearing mode SIF on the two sides of the specimen. For this reason in Tab. 1, KIII SIF values represent the edge values of crack front, since KIII SIF values are zero at the center of the crack front.

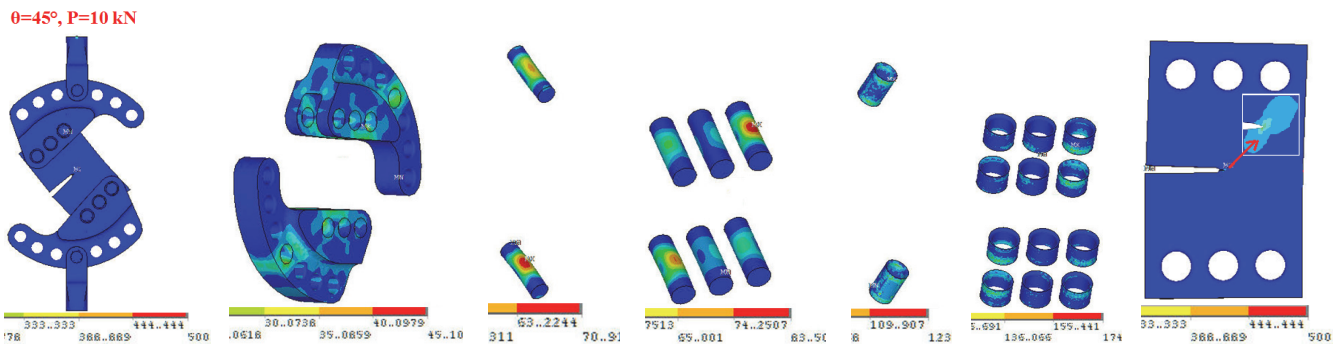


Figure 8: Stress distributions of mixed mode-I/II clevises, pins, bushes and specimen under 10 kN load value and  $45^\circ$  loading angle.

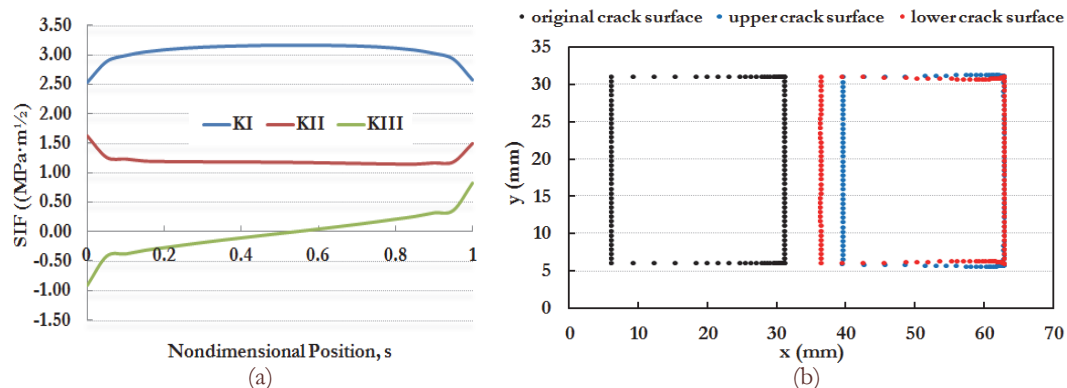


Figure 9: (a) Variation of SIF values obtained along the crack front, (b) Original crack surface before applying the load and upper and lower crack surfaces after applying the load - 10 kN load value and  $45^\circ$  loading angle.

25 mm-thick CTS specimens are used in numerical fracture analyses for all loading angles. However, in experimental analyses, 10 mm-thick specimens are used because of the high load requirements for 25 mm thickness. Therefore, numerical analysis results for 25 mm thick are scaled to represent 10 mm thickness. To prove the scaling procedure, SIF values along the crack front of 25 mm-thick and 10 mm-thick CTS specimens are given in Fig. 10. It can be seen from Fig. 10 that mode-I and mode-II SIFs linearly change with specimen thickness.

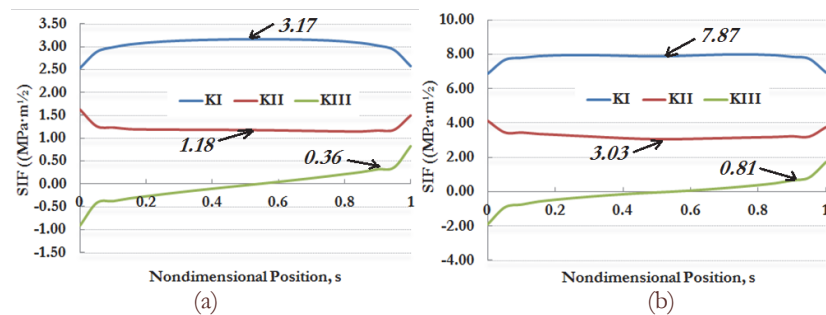


Figure 10: Variation of SIF values along the crack front of CTS specimens, (a) 25 mm thickness, (b) 10 mm thickness.

In Fig. 11, variations of KI, KII and KIII SIF values along crack front for all loading angles are given. It is seen that, as expected, KII and KIII increase with increasing loading angle while KI decreases. KII and KIII are equal to zero for  $0^\circ$  and KI is equal to zero for  $90^\circ$  loading angle.

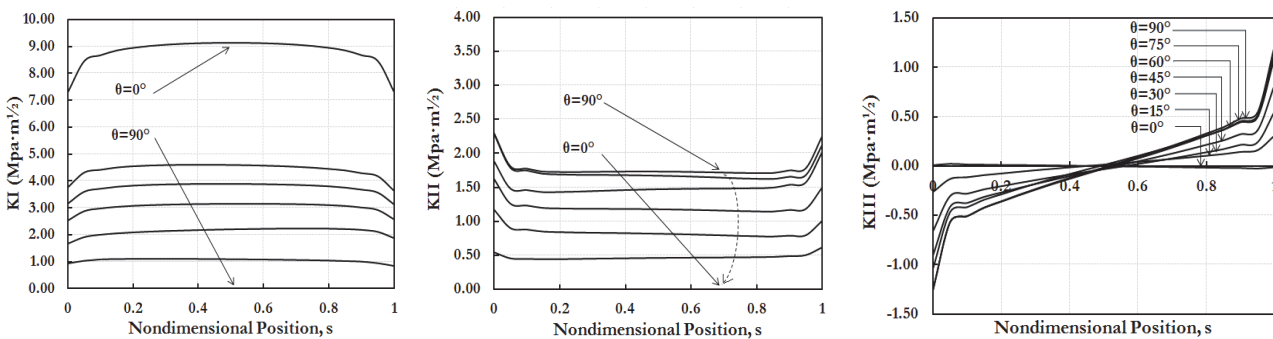


Figure 11: Variations of KI, KII and KIII SIF values along crack front for all loading angles.

## EXPERIMENTAL STUDIES ON MODE-I/II FRACTURE

This section deals with experimental studies on mode-I/II fracture tests. In the first subsection, details of the experimental set-up, including materials and equipment used, specimen preparation and testing procedure, are explained. The second subsection contains experimental results in terms of fracture loads, crack lengths and broken samples for all the tests performed.

### Description of The Experimental Set-Up

The experiments are performed on 100 kN "Schimadzu Servo Pulser" axial fatigue test machine and 200 kN "Schimadzu AG-X Plus" tensile test machine. In Fig. 12, overall views of the experimental set-up and the equipment used are shown. As seen from this figure, the test assembly consists of mode-I/II CTS and T-specimen (Al 7075-T651), the loading apparatus (St 4140), the pins (HSS steel) and a camera.

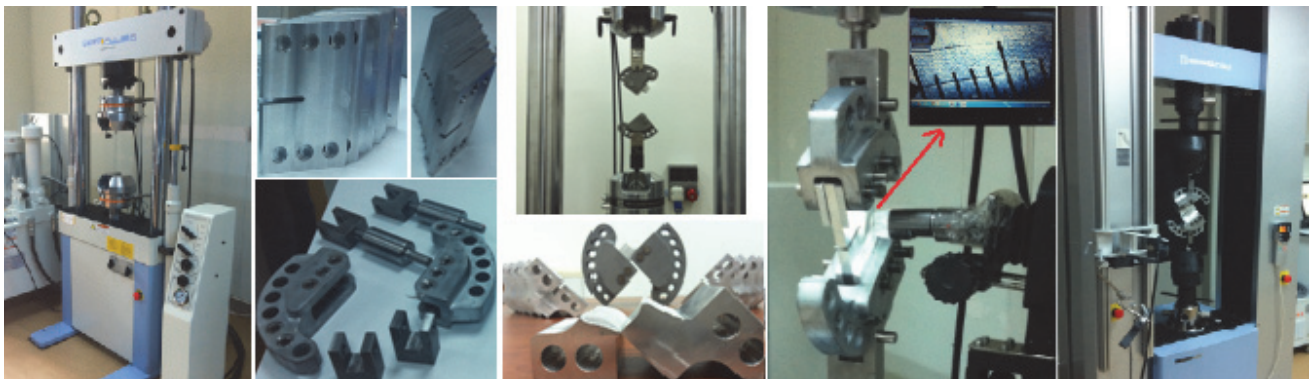


Figure 12: Overall views of the experimental set-up, the equipment and test machines used.

Before tensile load application, fatigue pre-cracking is performed under mode-I loading for all CTS specimens according to ASTM E399 standard [19] by using axial fatigue test machine. Pre-crack lengths of all CTS specimens used in experiments are determined as indicated in the standard (Pre-crack Length  $\geq 0.025W$  or 1.3 mm whichever is larger) and crack propagation is monitored and controlled by using a high-zoom camera. Also pre-crack load is determined according to the ASTM condition ( $K_{max} \leq 0.8K_Q$ ). After generation of the pre-crack, tensile load is applied to CTS specimens under different loading angles. Tensile load rate is applied by taking account of standard limitations that is given as follows,  $0.55 \text{ MPa}\sqrt{\text{m}}/\text{s} \leq \Delta K/\Delta t \leq 2.75 \text{ MPa}\sqrt{\text{m}}/\text{s}$ . Finally, load-displacement data are taken from the machine and critical fracture load is determined as indicated in the standard. Taking into account the above-mentioned considerations fracture tests are also performed for the T-specimens.

### Results of CTS Specimen Experiments

In this subsection, results from the mixed mode fracture tests of CTS specimen are presented for different loading angles. Tab. 2 summarizes different cases tested. Critical fracture loads are determined from load-displacement curves according

to the standard and crack deflection angles are measured from the fracture surfaces. Also, a 25 mm-thick CTS specimen is tested for  $30^\circ$  loading angle and its results are given in the table.

Specimen No	Specimen Type	Loading Angle ( $^\circ$ )	Thickness (mm)	Crack Length (mm)	Pre-crack Load (kN)	EXPERIMENTAL	
						Critical Load (kN)	Crack Deflection Angle ( $^\circ$ )
LT-01-150814-01	CTS	0	10.00	46.50	6.5	11.38	0.00
LT-01-251214-01	CTS	15	10.07	46.07	6.5	26.11	-9.41
LT-01-251214-02	CTS	15	10.06	45.96	6.5	26.68	-8.75
LT-01-150814-02	CTS	30	9.60	45.08	6.5	27.52	-26.85
LT-01-150814-03	CTS	30	10.10	44.94	6.5	28.59	-25.36
LT-01-150814-04	CTS	30	10.20	45.03	6.5	29.57	-26.42
LT-01-090215-01	CTS	30	25.00	46.51	6.5	60.23	-26.57
LT-01-150814-06	CTS	45	10.13	44.95	6.5	35.61	-35.71
LT-01-150814-07	CTS	45	10.17	44.75	6.5	33.00	-36.03
LT-01-220814-11	CTS	45	10.13	45.40	6.5	35.60	-36.54
LT-01-150814-09	CTS	60	10.16	44.93	6.5	46.25	-41.18
LT-01-150814-10	CTS	60	10.15	45.22	6.5	46.90	-41.11
LT-01-150814-12	CTS	60	10.18	45.20	6.5	45.71	-
LT-01-251214-03	CTS	75	10.10	46.38	6.5	62.73	-50.66
LT-01-150814-04	CTS	75	10.14	45.24	6.5	68.07	-53.64

Table 2: Experimental results of CTS specimen obtained from the mixed mode fracture tests.

In Fig. 13, overall view of fracture surfaces from broken samples under  $45^\circ$  loads are given. As can be seen from Tab. 2 and Fig. 13, consistent fracture surfaces and deflection angles are observed from the tests for all loading angles.



Figure 13: Overall broken sample pictures and fracture surfaces of CTS specimen for  $45^\circ$  loading angle.

Load-displacement curves and critical fracture load values for  $45^\circ$  loading angle are also given in Fig. 14. The critical fracture load is determined according to curve types listed in the ASTM E399 standard [19]. The procedure mentioned above is performed for all loading angle cases and obtained fracture loads are compared with some of the existing mode-I/II fracture criteria and are used to new mode-I/II fracture criterion.

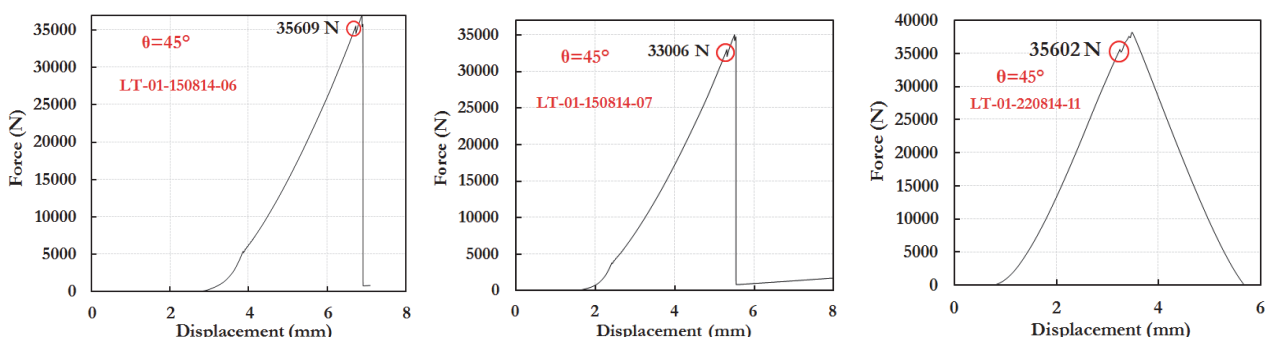


Figure 14: Load-displacement curves of CTS specimen for  $45^\circ$  loading angle after fracture tests.



### Results of T-Specimen Experiments

In this subsection, results from mixed mode fracture analyses of a new type of mixed mod-I/II specimen, T-specimen, that has smaller dimensions compared to the regular CTS specimen are presented. In Fig. 15, front and overall views of the T-specimen and its loading devices are shown. Detailed fracture analyses are performed using different dimensions under different loading cases to provide small scale yielding conditions under LEFM rules. Crack tip plastic zone sizes of all specimens are measured after the fracture analyses to make sure that plastic zone size is smaller than 1/50 of the specimen thickness for all loading cases.

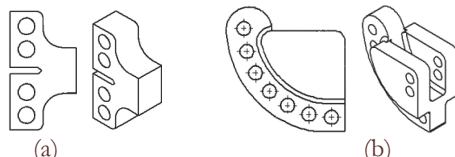


Figure 15: The front and overall views of (a) T-specimen, (b) Loading device of the specimen.

Overall views of the mixed mode-I/II test assembly solid model and of T-specimen along with experimental set-up for 45° loading angle are given in Fig. 16. Mixed mode loading clevises are designed such that for all loading angles, the loading axis to pass through the mid-point of a line that can be drawn between the inner two pins.

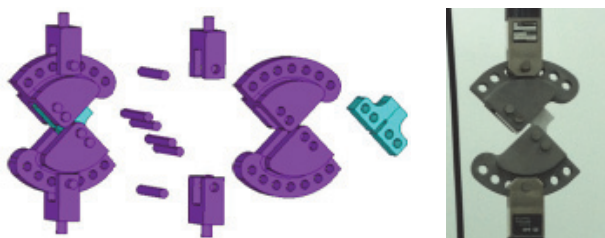


Figure 16: Overall and exploded views of the T-specimen test assembly and experimental set-up (loading angle 45°).

Tab. 3 summarizes experimental results from 25 mm-thick T-specimen tests. It can be seen from the experimental results of CTS and T specimens that loading requirements of 25 mm thick T specimens under all loading cases are lower than 10 mm thick CTS specimens.

Specimen No	Specimen Type	Loading Angle (°)	Thickness (mm)	Crack Length (mm)	Pre-crack Load (kN)	EXPERIMENTAL	
						Critical Load (kN)	Crack Deflection Angle (°)
T-LT-01-251214-01	T	0	24.87	26.03	10.5	19.60	0.00
T-LT-01-180115-12	T	15	25.00	26.93	10.5	19.80	-11.73
T-LT-01-180115-13	T	15	24.98	26.34	10.5	19.70	-9.34
T-LT-01-180115-14	T	30	24.98	26.21	10.5	23.07	-21.95
T-LT-01-180115-15	T	30	25.00	26.90	10.5	20.64	-18.07
T-LT-01-251214-02	T	45	25.00	25.24	10.5	28.09	-26.26
T-LT-01-251214-03	T	45	25.01	25.46	10.5	29.21	-24.15
T-LT-01-251214-04	T	60	24.96	27.13	10.5	33.59	-33.69
T-LT-01-090215-18	T	60	25.00	26.58	10.5	34.76	-36.41
T-LT-01-180115-17	T	75	25.03	26.89	10.5	54.31	-50.19
T-LT-01-220215-22	T	75	24.96	26.70	10.5	55.04	-53.17

Table 3: Experimental results of T-specimen.

## CONCLUSIONS

In this study, numerical and experimental analyses were performed using CTS specimen under different mixed mode-I/II loading. A new specimen type together with its loading device was also proposed that has smaller dimensions compared to the regular CTS specimen. Experimental results for the new specimen under different loading cases



were also presented. The results showed that the new specimen can be used as a practical test configuration for mixed mode-I/II fracture investigations. In Part 2 of this study, fracture experiments of the finite element models of CTS and T-specimen are conducted to check the validity of some of the existing criteria for mixed mode-I/II fracture conditions and to develop a further refined mode-I/II fracture criterion.

## ACKNOWLEDGEMENTS

The financial support by The Scientific and Technological Research Council of Turkey (TÜBİTAK) for this study under project no 113M407 and the ability of usage of axial fatigue machine at Bursa Technical University for the experiments are gratefully acknowledged.

## REFERENCES

- [1] Erdogan, F., Sih, G.C., On the Crack Extension in Plane Loading and Transverse Shear, *J. Basic Eng.*, 85 (1963) 519–527.
- [2] Sih, G.C., Macdonald, B., Fracture Mechanics Applied to Engineering Problems-Strain Energy Density Fracture Criterion, *Eng. Fract. Mech.*, 6 (1974) 361–386.
- [3] Nuismer, R.J., An energy release rate criterion for mixed mode fracture, *Int. J. Fatigue*, 11 (1975) 245–250.
- [4] Hussain, M.A., Pu, S.U., Underwood, J., Strain energy release rate for a crack under combined mode I and II, *ASTM STP*, 560 (1974) 2–28.
- [5] Chang, K.J., On the maximum strain criterion—A new approach to the angled crack problem, *Eng. Fract. Mech.*, 14 (1981) 107–124.
- [6] Koo, J.M., Choy, Y.S., A new mixed mode fracture criterion: maximum tangential strain energy density criterion, *Eng. Fract. Mech.*, 39 (1991) 443–449.
- [7] Pook, L.P., The significance of mode I branch cracks for mixed mode fatigue crack growth threshold behaviour. In: Brown, M.W., Miller, K.J., (eds), *Biaxial and multiaxial fatigue*, *Mech. Engng. Publ.*, London, (1989) 247–263.
- [8] Tanaka, K., Fatigue crack propagation from a crack inclined to the cyclic tensile axis, *Engng. Fract. Mech.*, 6 (1974) 493–507.
- [9] Ayatollahi, M.R., Aliha, M.R.M., Analysis of a new specimen for mixed mode fracture tests on brittle materials, *Eng. Fract. Mech.*, 76 (2009) 1563–1573.
- [10] Arcan, M., Hashin, Z., Voloshin, A., A method to produce uniform plane stress states with applications to fiber reinforced materials, *Exp. Mech.*, 18 (1978) 141–6.
- [11] Richard, H.A., Benitz, K., A loading device for the creation of mixed mode in fracture mechanics, *Int. J. Fracture*, 22 (1983) R55-R58.
- [12] Richard, H.A., Theoretical crack path determination, *Int. Conf. on Fatigue Crack Paths*, Parma (Italy), (FCP 2003), conference chairmen: A. Carpinteri, L.P. Pook.
- [13] Richard, H., Fracture mechanical predictions for cracks with superimposed normal and shear loading, Düsseldorf: VDI-Verlag; (1985) [in German].
- [14] Richard, H.A., In: *Structural failure, product liability and technical insurance*, Rossmanith (Ed.), Inderscience Enterprises Ltd., Genf., (1987).
- [15] ANSYS, Theory Manual Version 9.0. Ansys Inc., Canonsburg, PA, USA. (2004).
- [16] Ayhan, A.O., Nied, H.F., Stress intensity factors for three-dimensional surface cracks using enriched elements, *Int. J. Numer. Method Engng.*, 54 (2002) 899–921.
- [17] Ayhan, A.O., Nied, H.F., FRAC3D—Finite element based software for 3-D and generalized plane strain fracture analysis, SRC Tech. Report, (1998).
- [18] Demir, O., Dündar, H., İriç, S., Ayhan, A.O., Three-Dimensional Fracture Analyses of Compact Tension Shear Specimen Under In-Plane Mixed Mode Loading, UKK 10th Int. Fracture Conf., 24-26 April, Kayseri, Turkey, (2014).
- [19] ASTM International, E399 – 12, Standard Test Method for Linear-Elastic Plane-Strain Fracture Toughness KIc of Metallic Materials, (2013).